The Catalan Light Cone:
Dyck Paths as a Discrete Substrate for Causal Geometry, Quantum Amplitudes, and Computation

Paul Fernandez

Abstract

We study the Catalan family of structures—Dyck paths, full binary trees, and balanced parenthesis expressions—as a single discrete space of admissible histories with multiple equivalent "coordinate systems." The Dyck constraint induces a natural causal prefix order, and organizing histories by tier and lateral spread yields a discrete cone whose extremal configurations reproduce a light-cone–like causal envelope.

Classical results on conditioned random walks imply that, under diffusive scaling, Dyck ensembles converge to Brownian excursions. This provides a continuum comparison in which the induced evolution is governed by the heat operator on the half-line (with the Dyck conditioning encoded by boundary conditions, or equivalently by conditioning), and under analytic continuation one obtains the free Schrödinger equation.

The same Catalan shapes also serve as unlabeled application skeletons for λ-calculus and SKI terms (after choosing a standard finite encoding of symbols). Under this reading, causal extension aligns with functional application while local collapse aligns with computational reduction. We also present a minimal amplitude construction: given an observable/coarse-graining f and an additive phase functional (e.g. Dyck area), coherent summation over the preimages $f^{-1}(x)$ produces interference under Born-style squaring.

Throughout, we distinguish rigorously established statements (combinatorics, scaling limits, and commutation of disjoint local rewrites) from interpretive or open extensions (measurement, interactions, constants).

1 Introduction

Discrete approaches to fundamental physics suggest that continuum spacetime and quantum dynamics may emerge from deeper combinatorial structure. Examples include causal sets [5], discrete random surfaces and Causal Dynamical Triangulations (CDT) [2, 3], spin networks and loop quantum gravity [15], tensor networks [13], and rewriting systems inspired by λ-calculus and combinatory logic.

Typically, however, these models require multiple independent ingredients: a relation or graph for causal structure, an algebra for computation, and additional rules for quantum propagation. This work explores a more economical possibility: that a *single* recursive structure simultaneously supports all three.

The focus is the *Catalan substrate*, the family of structures counted by the Catalan numbers [16], including Dyck paths, full binary trees, and balanced parenthesis expressions. These objects are usually studied in enumerative combinatorics, probability theory, and theoretical computer science. Here they are treated instead as a space of *admissible histories* generated by a minimal growth constraint.

One object, three coordinate systems. We will move freely between three canonically bijective Catalan families:

- Dyck paths (a constrained nearest-neighbour walk),

- full binary trees (recursive branching structure),

- parenthesis/pairs encodings (a linear trace of the same tree).

Switching between these views is not a simulation; it is a change of representation of the same underlying object. Each view foregrounds different structure: Dyck paths make causal order and scaling limits transparent; trees make locality and computation transparent; and pairs encodings make uniform syntax convenient.

Contributions and scope. The paper isolates a common structural core shared by three domains:

(i) **Causal geometry:** the prefix order on Dyck prefixes induces a discrete causal structure and a cone-shaped envelope with sharp extremals.

(ii) **Continuum comparison:** classical conditioned-walk results yield a diffusion limit (Brownian excursion, heat equation on the half-line), and an analytic-continuation bridge to the free Schrödinger equation [12, 10, 9, 11].

(iii) **Computation:** Catalan tree shapes provide unlabeled application skeletons for standard Turing-complete functional calculi (after choosing a finite encoding of symbols), and local reductions remain internal to the same family [6, 8, 4].

(iv) **Amplitudes:** given a coarse-graining (observable) and an additive phase functional, coherent summation over indistinguishable histories produces interference under Born-style squaring.

We do not attempt to derive interactions, constants, or a unique measurement postulate; where additional structure is introduced (e.g. complex phases and Born-style probabilities), it is presented as a minimal construction layered on the Catalan kinematics.

Organization. Section 2 establishes the discrete causal geometry of the Catalan lattice and its interpretation as a light cone. Section 3 develops the computational correspondence via binary application trees and pairs encodings. Section 4 introduces a minimal amplitude construction and the continuum comparison to diffusion and Schrödinger dynamics.[1] Locality and disjoint-commutation are discussed in Section 5. Optional coordinate embeddings, technical notes, and illustrative examples are collected in appendices, separate from the main formal development.

2 The Catalan Light Cone as a Discrete Causal Geometry

2.1 Dyck paths and growth tiers

A Dyck path of semilength n is a walk on the integers satisfying

$$H_{k+1} = H_k \pm 1, \qquad H_k \geq 0, \qquad H_0 = H_{2n} = 0.$$

---

[1]Depending on reader background, Sections 3 and Section 4 may be read in either order after the geometric setup in Section 2.

Equivalently, Dyck paths are balanced parenthesis strings or full binary trees with n internal nodes. The number of such paths is the nth Catalan number

$$C_n = \frac{1}{n+1}\binom{2n}{n}.$$

Each up–down pair () represents a minimal unit of growth. The integer n will be called the *tier* and will be interpreted as a discrete proper time.

2.2 Prefix order and causality

Let $\mathcal{C}$ denote the set of *Dyck prefixes*: balanced-parentheses prefixes that never go below height 0. Define a partial order by extension: $u \preceq v$ iff u is a prefix of v. We interpret this order as a causal relation: $u \preceq v$ means that u lies in the causal past of v, while prefixes that diverge represent incompatible futures. This prefix order defines a discrete causal structure:

- every node has a unique causal past,

- multiple incompatible futures may branch from the same prefix,

- cycles are prohibited by construction.

No additional causal axiom is introduced; causality is enforced combinatorially by the Dyck constraint.

2.3 Extremal configurations: chain and star

At fixed tier n there are many Dyck paths. Two extremal configurations play a distinguished role:

- the *chain* (or spine)
$$(((\cdots))),$$
fully nested, with maximal depth and minimal spread;

- the *star*
$$()()()\cdots(),$$
fully separated, with minimal depth and maximal spread.

All other configurations interpolate between these extremes. Together, the set of Dyck paths at tier n forms a discrete envelope bounded by the chain and the star.

2.4 Breadth as spatial extent

Define the *breadth* $r(w)$ of a Dyck path w to be the size of a largest level set in the associated full binary tree:

$$r(w) := \max_{\ell}\{\text{number of nodes at depth } \ell\}.$$

Equivalently, $r(w)$ is the maximal number of non-overlapping pairs at a common nesting depth. For a Dyck word of tier n there are n matched pairs in total, so

$$1 \le r(w) \le n,$$

with $r = 1$ for the fully nested chain and $r = n$ for the fully separated star. The inequality

$$r \le n$$

is enforced purely by the recursive constraint. It is the discrete analogue of the relativistic light-cone bound $|\Delta x| \le \Delta t$ (in units with $c = 1$).

Figure 1: The Catalan light cone. Tier n (the number of Dyck units) plays the role of proper time, while breadth r measures spatial radius. All Dyck configurations at fixed tier lie between the fully nested chain (timelike extreme) and the fully separated star (lightlike envelope). Discrete Dyck layers approximate constant-time hypersurfaces, and the bound $r \leq n$ is enforced combinatorially.

2.5 Depth–breadth tradeoff

Let $h(w)$ denote the maximum height of a Dyck path, i.e. the maximum nesting depth of its associated full binary tree (root at depth 0). Recall that the breadth $r(w)$ is the maximum number of nodes occurring at any fixed depth level:

$$r(w) := \max_{\ell} \text{number of nodes at depth } \ell.$$

Depth and breadth are not independent. In any full binary tree, the number of nodes at depth ℓ is at most 2^{ℓ} (each level can at most double from its parent level). Hence, if the maximum level set size $r(w)$ occurs at depth ℓ_*, then

$$r(w) \leq 2^{\ell_*} \leq 2^{h(w)} \quad \Rightarrow \quad h(w) \geq \log_2 r(w).$$

Thus configurations with large breadth necessarily have logarithmically large depth. Equivalently, very shallow trees cannot support wide level sets, while trees with very large depth must concentrate most nodes away from any single breadth-maximizing level.

Remark 2.1 (Kraft equality for leaf depths). *For the full binary tree associated to a Dyck path, if L is the set of leaves and $d(\ell)$ denotes the depth of $\ell \in L$ (root at depth 0), then*

$$\sum_{\ell \in L} 2^{-d(\ell)} = 1.$$

Equivalently, the leaf depths form a complete binary prefix code. This gives a global constraint on allowable depth profiles beyond the crude level bound $r(w) \leq 2^{h(w)}$; see [7].

2.6 Cone structure

Organizing Dyck paths by tier n and breadth r yields a discrete cone:

- each tier is a "constant-time" slice,
- the chain defines the timelike axis,

4

$$(((()))) \qquad (h = 3, \ r = 1)$$
$$(()()) \qquad (h = 2, \ r = 2)$$
$$(())() \qquad (h = 2, \ r = 2)$$
$$()(()) \qquad (h = 2, \ r = 2)$$
$$()()() \qquad (h = 1, \ r = 3)$$

Figure 2: All Dyck words of tier $n = 3$, ordered from maximal nesting (chain) to maximal separation (star). These five configurations exhaust the discrete causal possibilities at fixed proper time. Depth h and breadth r interpolate between the two extremes, illustrating the intrinsic tradeoff enforced by the Dyck constraint. Higher tiers replicate this structure at larger scale.

- the star defines the lightlike boundary,

- admissible configurations fill the interior.

This structure will be referred to as the *Catalan light cone*.

2.7 Scaling behavior

Classical results on conditioned random walks show that typical Dyck paths at tier n have height and breadth of order $\sqrt{n}$ [12, 10, 1]. Extremal configurations saturate the linear bound $r \leq n$, while typical configurations lie deep within the cone. This separation between extremal and typical behavior mirrors the role of null, timelike, and spacelike trajectories in relativistic geometry.

Theorem 2.1 (Discrete light-cone bound and scaling)**.** *Let w be a Dyck word of semilength n and breadth $r(w)$ as above. Then*
$$1 \leq r(w) \leq n.$$

Moreover, for a uniformly random Dyck word of semilength n, the typical height and breadth are of order $\sqrt{n}$.

The first statement follows from the definition of $r(w)$ and the fact that there are n internal nodes, while the scaling behavior is a consequence of invariance-principle results for conditioned random walks [12, 10, 1].

Coordinate charts and continuum comparisons. Appendix A collects optional coordinate-chart constructions (null-count embeddings and related continuum comparisons) used for intuition; the combinatorial results below do not depend on these embeddings.

2.8 Recursive Self-Similarity and Local Re-Centering

A key structural property of the Catalan substrate is its *recursive self-similarity*. Every Dyck word may be viewed as a node in the infinite prefix tree of admissible Dyck prefixes. At any such node u, with current height h and remaining length budget sufficient to return to height 0, the set of all admissible continuations of u forms a subtree whose shape is determined entirely by h. This subtree is canonically isomorphic to the Dyck-prefix tree that begins at height h rather than at height 0.

Formally, let $\mathcal{C}$ denote the Dyck-prefix tree (the poset of Dyck prefixes under extension) and $\mathcal{C}_h$ denotes the Dyck-prefix tree conditioned to start at height h (i.e. with $H_0 = h$ and $H_k \geq 0$ for all k), then for every prefix u of height h we have a canonical isomorphism

$$\mathcal{C}(u) \cong \mathcal{C}_h.$$

Thus every node of the global Catalan possibility tree is the root of a scaled copy of the entire admissible-future structure, with scaling determined solely by local height. The recursive decomposition of full binary trees,

$$T = \bullet(T_L, T_R),$$

makes the same fact explicit in the tree representation: each subtree of a Catalan tree is itself a Catalan tree, and the decomposition applies inductively at every depth.

This recursive self-similarity has two important consequences for the geometric interpretation developed in this paper:

(i) **Locality and re-centering.** Because the admissible future of any prefix depends only on its present height, not on its global position, the Catalan light-cone geometry is *locally homogeneous*. The causal cone may be re-centered at any node without altering its shape: moving the focus does not change the structure of admissible futures, only the value of the local height at which the cone is rooted.

(ii) **Scale invariance of the substrate.** The same recursive rules govern growth at every depth. The local possibility space looks the same at all scales, in the sense that the subtree below any node is again Catalan. This is the combinatorial source of the invariance principles (Dyck $\rightarrow$ Brownian excursion) appearing in the continuum limit.

In summary, the Catalan substrate is self-similar at every node: each point in the possibility space contains a full Catalan future scaled by its current height. This allows the causal and geometric analysis of later sections to be performed relative to *any* node of the prefix tree. The light cone is not anchored to a global origin; it is an intrinsic, relocatable geometric feature of the recursive structure itself.

2.9   Multiple Local Cones and Relational Geometry

The same prefix order that defines causality also yields a family of *local cones*: every Dyck prefix $u \in \mathcal{C}$ induces a future $\mathcal{C}(u)$ of admissible extensions, i.e. the same growth law re-centered at u. Two prefixes u and v relate in exactly two ways:

(i) **Nested cones.** If $u \preceq v$, then $\mathcal{C}(v) \subseteq \mathcal{C}(u)$.

(ii) **Divergent cones.** If neither prefix contains the other, then u and v share a maximal common prefix w and have disjoint futures beyond w.

Thus the cone picture is relocatable: it appears at every node, cones nest along causal chains, and branching produces incompatible futures.
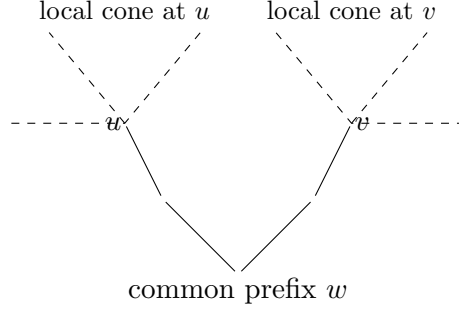
Figure 3: Two Dyck prefixes u and v diverging from a shared ancestor w. Dashed regions indicate the local Catalan cones rooted at u and v. Cones nest along causal chains and diverge after branching points, producing a family of local, relocatable causal geometries on the Catalan substrate.

2.10 Summary

The Catalan substrate supports a discrete causal geometry determined entirely by recursive constraint. Without introducing a manifold, metric, or causal relation by fiat, it yields:

- a partial order interpretable as causality,

- a cone-shaped causal envelope,

- intrinsic bounds on spatial extension,

- well-defined constant-time layers.

Subsequent sections place dynamical rules—quantum amplitudes and computational reduction—on this geometry.

3 Recursive Pairing and Universal Computation

We now read the same Catalan objects from the computational side. Full binary trees serve as application frames, while pairs encodings provide a uniform parenthesis-only syntax. The only additional choice needed to represent concrete programs is an encoding of symbols at leaves.

3.1 Pairs expansion

Catalan shapes as program frames. The Catalan family—Dyck paths, full binary trees, and balanced-parenthesis expressions—forms the free magma on a single binary constructor: it is the space of all finite binary application frames. As observed in classical treatments of the λ-calculus and combinatory logic [8, 4], application is binary, so every SKI term (and every λ-term after fixing a binding convention) has a canonical representation as a finite binary application tree: internal nodes encode application; leaves encode atomic symbols (variables, constants, or combinators). Conversely, any finite binary tree equipped with leaf labels denotes a unique applicative term over that alphabet, modulo surface syntax. Since SKI is computationally universal, this yields an explicit embedding of all computable programs (as terms) within the Catalan substrate. The apparent choice of leaf alphabet can itself be internalized by representing symbols as distinguished Catalan motifs (Remark 3.1).

Remark 3.1 (Symbols as Distinguished Motifs). *Although we sometimes describe leaf labels as an external choice, one may work in a purely structural setting: there is an injective encoding of labeled application trees (and in particular SKI terms) into unlabeled Catalan trees by tagging constructor nodes and representing each symbol by a fixed subtree motif. See Lemma D.1 in Appendix D.*

This observation also extends to operational semantics. Standard reductions (such as β-reduction or SKI contraction) are local rewrite rules on binary trees, and the pairs-expansions of combinators remain within the Catalan family. Accordingly, a program, its intermediate expansion frames, and each permissible reduction schedule are all representable as paths through a single Catalan substrate. Selecting a program shape or selecting a specific reduction history is therefore equivalent to selecting a path in the Catalan tree. In this sense the Catalan substrate uniformly encodes program syntax, program semantics, and the full ensemble of admissible computational histories.

Proposition 3.1 (Catalan Universality for Program Structure). *Let $\mathcal{C}$ denote the Catalan family of finite full binary trees. Every program in any Turing-complete functional calculus (such as the λ-calculus or SKI) admits a canonical representation as an element of $\mathcal{C}$ with leaf labels drawn from a finite alphabet (after fixing a standard encoding of symbols). Conversely, every labeled element of $\mathcal{C}$ denotes a unique program modulo surface syntax. Furthermore, standard operational semantics (including β-reduction and SKI contraction) act as local rewrite rules that preserve membership in $\mathcal{C}$. Thus a program, its syntactic expansions, and every admissible reduction history correspond to paths within the Catalan substrate.*

A proof sketch is provided in Appendix D.

Two canonical parenthesis encodings. There are (at least) two particularly useful parenthesis-only encodings of a full binary tree:

- **Dyck encoding** ("walk" view): balanced parentheses of length $2n$, naturally adapted to height profiles and scaling limits.

- **Pairs (S-expression) encoding** ("cons" view): write each leaf as () and each internal node as a parenthesized pair of its two children, i.e. $T = (L, R) \mapsto (\texttt{enc}(L)\,\texttt{enc}(R))$. This is a variable- and label-free Lisp-style representation with () as the only atom.

In particular, in the *pairs* encoding, the smallest object is the empty pair (), and the smallest nontrivial *binary* object is (()()), i.e. a root pair whose two children are leaves. In the Dyck encoding, the semilength-1 object is (), since Dyck words begin only after the first matched pair exists.

3.2 A small tier shown three ways (Dyck / tree / pairs)

Figure 4 augments the standard Dyck-$n = 3$ list by displaying, for the *same* five Catalan shapes, the corresponding pairs (S-expression) encodings.
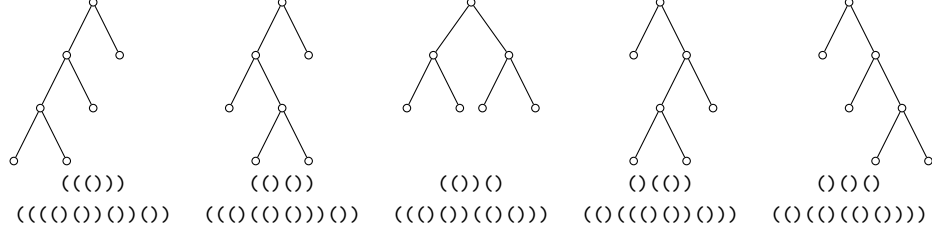
8

Figure 4: The five Catalan shapes at tier $n = 3$ shown as (i) Dyck words, (ii) full binary trees, and (iii) pairs (S-expression) encodings in which each leaf is () and each internal node is a parenthesized pair of its two children (as if one were looking "down into" the tree). These are three coordinate systems for the same underlying Catalan objects.

3.3   Connection to λ-calculus and SKI

Full binary trees are a standard representation of SKI terms, and they capture the application skeleton of λ-terms [6, 8, 4]. A full λ-encoding requires a binding convention (e.g. variables as leaf labels or positions, and abstraction as a structural marker), while application is encoded by the tree's binary node. Under the pairs expansion, each Dyck tree canonically determines an unlabeled application graph. When variables are suppressed, the resulting graphs coincide with the structure graphs used in combinatory logic. No additional primitives beyond recursive pairing are required to obtain this representation.

Choosing a finite set of tree patterns to represent the SKI combinators and interpreting local tree rewrites as SKI reduction therefore equips the Catalan substrate with a standard universal calculus: every partial recursive function can be encoded as an SKI term [8, 4], and hence by a finite Dyck tree, and every computation corresponds to a sequence of local tree transformations. In this sense, the Catalan substrate is *computationally universal*. What is new here is that the same underlying objects simultaneously carry a causal and geometric interpretation.

3.4   Reduction and local collapse

In the computational interpretation, reduction corresponds to local pattern replacement. A redex occupies a finite region of a tree and may be reduced without reference to distant subtrees. This locality mirrors the causal structure established in Section 2. From the perspective of the Catalan lattice, reduction may be viewed as *collapse*: a locally ambiguous structure is replaced by a simpler one consistent with the global constraint. Importantly, collapse does not alter causal ancestry; it refines an already-admissible history. For standard calculi (e.g. λ/SKI), confluence ensures uniqueness of normal forms when they exist, and more locally reductions supported on disjoint subtrees commute. This computational fact will later support an interpretation of spacelike commutativity.

3.5   Summary

Recursive pairing suffices to encode universal computation. Via the pairs expansion, Dyck trees and application graphs are two views of the same structure. Local computational reduction aligns naturally with causal locality on the Catalan light cone.

4 Quantum Amplitudes on the Catalan Lattice

This section layers a minimal amplitude calculus on the Catalan history space. The key inputs are (i) a coarse-graining/observable f identifying which histories are regarded as the same outcome, and (ii) a choice of additive phase functional on histories. Given these, we define amplitudes by coherent summation over preimages and probabilities by normalized squared magnitudes, in analogy with the Born rule [9].

4.1 Histories as paths

Interpreting Dyck paths as admissible histories motivates assigning weights to each history. Let $\mathcal{D}_n$ denote the set of Dyck paths of tier n. A state at tier n may be represented as a formal superposition of histories

$$\Psi_n = \sum_{w \in \mathcal{D}_n} \psi(w) \, |w\rangle.$$

Local extensions of a Dyck path correspond to admissible future steps. Thus, time evolution is governed by transitions that respect the Dyck constraint.

4.2 Observables, projection, and coherent summation

Fix a tier n and consider the set $\mathcal{D}_n$ of Dyck paths of semilength n. Each $w \in \mathcal{D}_n$ represents a complete admissible history at discrete time n, with an associated height profile

$$H_w : \{0, 1, \ldots, 2n\} \to \mathbb{Z}_{\geq 0}.$$

An observable is defined as a deterministic coarse-graining

$$f : \mathcal{D}_n \to \mathcal{X},$$

where $\mathcal{X}$ is a discrete set of outcomes corresponding to a chosen equivalence relation on histories. An outcome $x \in \mathcal{X}$ corresponds to the equivalence class $f^{-1}(x) \subset \mathcal{D}_n$ of histories. By construction, such a projection discards information: many distinct histories may be identified as the same observable outcome.

With no additional structure imposed, the natural measure on $\mathcal{D}_n$ is uniform counting. The induced distribution on the outcome space $\mathcal{X}$ is therefore the pushforward of the uniform counting measure,

$$N(x) := \#\{w \in \mathcal{D}_n : f(w) = x\}.$$

Even with uniform weight on histories, the induced distribution on $\mathcal{X}$ is generically non-uniform, reflecting the combinatorial geometry of the projection rather than any imposed dynamics.

A discrete analogue of an integral along a history is given by the step-sum of the height profile,

$$A(w) := \sum_{k=0}^{2n-1} H_w(k),$$

which measures the cumulative dwell time at nonzero height. This quantity depends on the full distribution of height along the path, not merely on extrema such as maximum height or peak count.

More generally, one may use any *additive* functional on Dyck histories as a phase source, provided it is computable online from prefix-local growth information. The following proposition records the general form of such functionals.

Proposition 4.1 (Additive phase functionals computable along Dyck growth)**.** *Let w be a Dyck history of semilength n, and let $(X_t)_{t=0}^{2n-1}$ denote the sequence of* prefix-local *growth states along w (e.g. current height and step type). For Dyck histories u, v define concatenation uv as the concatenation of Dyck words.*

A real-valued functional $\Phi(w)$ is additive under Dyck concatenation, i.e. $\Phi(uv) = \Phi(u) + \Phi(v)$, and computable online by a (possibly countable-state) Markov transducer driven by (X_t) with fixed initial internal state $Y_0 = y_*$ for every history, if and only if there exist an internal state process (Y_t) with update rule $Y_{t+1} = F(Y_t, X_t)$ and a real-valued increment function g such that

$$\Phi(w) \;=\; \sum_{t=0}^{2n-1} g(Y_t, X_t).$$

Equivalently, defining the augmented prefix-local state $Z_t := (X_t, Y_t)$, one has

$$\Phi(w) \;=\; \sum_{t=0}^{2n-1} \varphi(Z_t)$$

for some function φ on the augmented state space.

Proof sketch. Immediate: an online additive transducer emits a per-step output $g(Y_t, X_t)$, whose sum over the growth process defines Φ; conversely, any such per-step sum is computable by an online transducer with internal state (Y_t). $\qquad\square$

Remark 4.1. *In the special case where the transducer carries no internal state (i.e. Y_t is trivial) and the prefix-local state is taken to be the current height h_t, the admissible phase functionals are precisely those of the form*

$$\Phi_f(w) = \sum_t f(h_t),$$

for some function $f : \mathbb{Z}_{\geq 0} \to \mathbb{R}$. Allowing dependence on step type yields the slightly more general form $f(h_t, \Delta h_t)$. The area functional corresponds to the choice $f(h) = h$.

Specializing to the area functional $A(w)$, one may define a complex phase

$$\theta(w) := \alpha \, A(w), \qquad \psi(w) := e^{i\theta(w)},$$

where α is a global scale parameter. No per-path phase assignment is introduced; distinct phases arise solely from differences in the distribution of height over the history.

Given an observable f, the complex amplitude associated with an outcome $x \in \mathcal{X}$ is the coherent sum

$$\Psi(x) := \sum_{w:\, f(w)=x} \psi(w),$$

and observed probabilities are obtained by normalization of squared magnitudes,

$$P(x) = \frac{|\Psi(x)|^2}{\sum_{x' \in \mathcal{X}} |\Psi(x')|^2}.$$

Thus histories that are indistinguishable under the observable f are combined prior to squaring, while distinguishable histories are not. Interference is therefore a generic consequence of assigning complex weights to histories and summing coherently over coarse-grained equivalence classes before applying the Born rule.

Optional: coarse-graining entropy.   Appendix B records an optional entropy bookkeeping for coarse-grainings and collapse counts.

4.3   Path integrals and conditioned walks

Dyck paths are random walks conditioned to remain nonnegative and return to zero. Classical results show that, when rescaled appropriately, ensembles of such paths converge to Brownian excursions [12, 10]. Assigning equal weight to all admissible paths yields a discrete analogue of a path integral [9]. More general amplitude assignments may depend on local features such as height or curvature, provided the Dyck constraint is preserved.
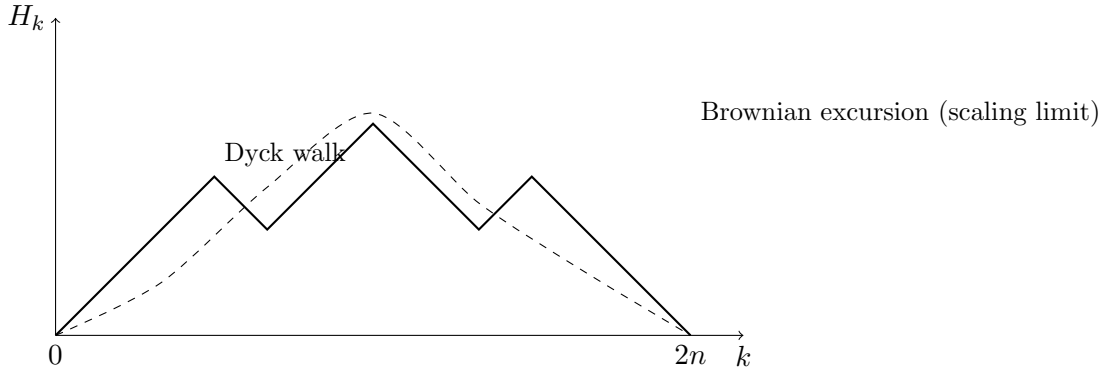

Figure 5: A Dyck path as a nearest-neighbour walk (H_k) constrained to stay nonnegative and return to zero at time $2n$. Under diffusive rescaling of k and H_k, ensembles of such paths converge to Brownian excursions, providing the bridge to the heat and Schrödinger equations discussed in the text.

4.4   Discrete path-integral formulation

The preceding constructions admit a direct interpretation as a discrete path integral on the Catalan light cone. Fix a tier n and an observable $f : \mathcal{D}_n \to \mathcal{X}$, where $\mathcal{X}$ is a finite set of outcomes corresponding to a chosen coarse-graining of histories. Each Dyck path $w \in \mathcal{D}_n$ represents a complete admissible history, and the projection f determines which distinctions between histories are retained and which are discarded.

Define a complex weight for each history by

$$\psi(w) = e^{i\alpha A(w)},$$

where

$$A(w) = \sum_{k=0}^{2n-1} H_w(k)$$

is the discrete height integral introduced above. The amplitude associated with an observable outcome $x \in \mathcal{X}$ is then

$$\Psi(x) = \sum_{w:\, f(w)=x} e^{i\alpha A(w)}.$$

This expression is formally analogous to a path integral [9]: the amplitude is a sum over all admissible histories compatible with the observable outcome, with each history contributing a

phase determined by an additive functional. No continuum limit, action functional, or variational principle is assumed at this stage; the structure arises purely from discrete combinatorics.

Several features commonly associated with continuum path integrals are already present:

(i) **Sum over histories.** All admissible Dyck paths consistent with the observable contribute. The Dyck constraint enforces causal admissibility in the same way that restrictions on allowed paths do in relativistic path integrals.

(ii) **Additive phase functional.**

The quantity $A(w)$ is additive under concatenation of path segments and depends only on the local height increments. It therefore plays the role of a discrete action accumulated along the history.

(iii) **Interference from coarse-graining.** Interference arises precisely because the observable f fails to distinguish between certain histories. Histories that are identified by the projection are summed coherently, while those distinguished by the observable are not.

From this perspective, the Catalan lattice provides a discrete realization of the sum-over-histories principle in which both the space of histories and the phase functional are combinatorially well defined. In the next subsection we show that, under appropriate scaling limits, this discrete formulation converges to familiar continuum descriptions governed by diffusion and Schrödinger dynamics.

Concrete physical measurements may be modeled by choosing observables that retain geometric features of a history (such as transverse displacement at a fixed tier). No such spatial interpretation, however, is required for the formal development.

For readers seeking a concrete intuition for how this discrete sum-over-histories mechanism produces interference, Appendix C sketches a finite thought experiment analogous to the double-slit experiment.

4.5   Scaling of the area phase in the continuum limit

The interference mechanism above assigns each history $w \in \mathcal{D}_n$ a complex weight $\psi(w) = e^{i\alpha A(w)}$ with discrete area functional

$$A(w) := \sum_{k=0}^{2n-1} H_w(k),$$

where $H_w(k)$ is the height after k steps.

To relate this discrete phase to the diffusion scaling limit, introduce the rescaled height process on $[0,1]$,

$$X^{(n)}(\tau) := n^{-1/2} H_w(\lfloor 2n\tau \rfloor), \qquad 0 \le \tau \le 1.$$

Under the standard Dyck-to-Brownian-excursion scaling, $X^{(n)} \Rightarrow X$ in distribution, where X is a Brownian excursion on $[0,1]$.

The discrete area rescales as a Riemann sum:

$$\frac{1}{2n^{3/2}} A(w) = \frac{1}{2n} \sum_{k=0}^{2n-1} n^{-1/2} H_w(k) \implies \int_0^1 X(\tau)\, d\tau.$$

Consequently, a nontrivial continuum phase is obtained by scaling α with n as

$$\alpha_n := \frac{\lambda}{2n^{3/2}},$$

13

so that

$$e^{i\alpha_n A(w)} \implies \exp\Big(i\lambda \int_0^1 X(\tau)\,d\tau\Big).$$

This makes explicit that the discrete coherent sum with additive functional $A(w)$ converges to a continuum functional weight. In particular, when one passes from uniform counting of conditioned walks to diffusion limits, inserting the exponential of a time-integrated functional corresponds (at the PDE level) to adding a potential term (via the standard Feynman–Kac mechanism [11]). Setting $\lambda = 0$ recovers the unweighted scaling limit discussed in the next subsection.

4.6   Diffusion limit

Let $n \to \infty$ and rescale time and height by

$$t \mapsto n\tau, \qquad h \mapsto \sqrt{n}\,x.$$

Under this scaling, the rescaled Dyck height process converges in law to a Brownian excursion on $x \geq 0$. At the PDE level, the diffusion part is governed by the heat operator on the half-line, while the Dyck constraint (nonnegativity and return) is implemented via conditioning and boundary data. In particular, on $x > 0$ one has a heat equation of the form

$$\partial_\tau \rho = \frac{1}{2}\,\partial_x^2 \rho, \tag{1}$$

See [12, 10] for standard derivations and precise statements. Appendix A, Section A.3 records a complementary view of the same limit through the covariance structure of the height observable and its Karhunen–Loève modes.

4.7   Schrödinger equation

More formally, if $\rho(\tau, x)$ denotes the real heat kernel on $x \geq 0$, analytic continuation in the diffusion parameter, $\tau \mapsto it$, produces a complex-valued kernel $\psi(t, x)$ satisfying the free Schrödinger equation

$$i\partial_t \psi = -\frac{1}{2}\,\partial_x^2 \psi. \tag{2}$$

Mode-wise phase.   Appendix A, Section A.3 shows that, after projecting Dyck histories to the height observable, the resulting signals admit a canonical eigenmode decomposition (Karhunen–Loève modes) of their correlation structure. In the continuum limit, the heat equation is diagonalized by the spectral decomposition of the half-line Laplacian (sine/cosine modes depending on boundary conditions), so each mode evolves by a real decay factor $e^{-k^2\tau/2}$. Under $\tau \mapsto it$ these become pure phases $e^{-ik^2t/2}$. In this sense, analytic continuation replaces diffusive decay by unit-modulus phase rotation of modal coefficients, making coherent cancellation and reinforcement stable under time evolution.

Boundary conditions at $x = 0$ are carried over from the diffusive regime (e.g. reflecting or absorbing), and the choice of boundary does not affect the existence of the continuum limit itself. Thus, quantum wave dynamics arises here as the analytic continuation of diffusive propagation on the Catalan lattice, in line with the classical connection between diffusion and Schrödinger evolution [9, 11]. No separate quantization procedure is required; the wave equation is inherited from the scaling limit of constrained combinatorial growth.

5 Locality and Disjoint Commutation

5.1 Disjoint subtrees

Two subtrees of a Dyck tree that share no common ancestor beyond a given prefix are causally independent. Operations localized to one subtree do not affect the other. In the computational interpretation, this corresponds to independent reductions. In the amplitude interpretation, it corresponds to commuting operators acting on spacelike-separated regions (an analogue of microcausality). Multiple fine-grained histories may represent the same abstract computation or the same coarse-grained outcome, differing only in the interleaving of independent local updates. When such differences are unobservable (or regarded as irrelevant bookkeeping), one may quotient the history space by the induced equivalence relation, replacing many interleavings by a single equivalence class. This redundancy is structurally analogous to gauge: distinct internal descriptions correspond to the same coarse description.

Operationally, fix an initial tree and consider histories that apply the same multiset of local reductions but differ only in the temporal ordering of reductions supported on disjoint subtrees. By Lemma D.2, these interleavings are related by commuting diamonds. One may therefore treat each equivalence class as a single abstract history (a partial order of events) while reserving genuinely different choices of which reductions occur for the nontrivial branching structure of the multiway reduction graph.
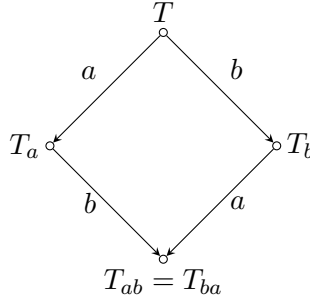

Figure 6: Local diamond for commuting disjoint updates. Starting from a common state T, two spacelike-separated reductions a and b can be applied in either order, yielding intermediate states T_a and T_b but the same final state $T_{ab} = T_{ba}$. The two intermediate events are spacelike-separated: they share a common past (T) and a common future (T_{ab}) but no causal edge between them. This expresses a microcausality analogue on the Catalan substrate: local updates supported on disjoint subtrees commute and differ only by temporal ordering.

(See Appendix D, and in particular Lemma D.2, for a formal statement and proof sketch of the corresponding disjoint-commutation property.)

5.2 Collapse and selection

Both computation and amplitude propagation require selection:

- computational reduction chooses a redex,

- measurement-like selection chooses an observable outcome, corresponding to an equivalence class under the chosen projection.

In the Catalan substrate, selection operates locally, refining rather than destroying structure. The global constraint ensures consistency after selection. The formal development of collapse probabilities lies beyond the scope of this paper and is treated here only structurally.

5.3 Summary

Locality and disjoint commutation emerge directly from the causal and recursive structure of the Catalan lattice. The same principles underlie both computational reduction and quantum amplitude constructions on the Catalan history space.

6 Discussion and Limitations

The results presented here establish a shared structural basis for causal geometry, quantum dynamics, and computation. Several limitations should be emphasized:

- Physical constants and interactions are not derived.

- Only free (noninteracting) wave dynamics appears explicitly.

- Collapse probabilities are not fixed uniquely by the structure.

- Lorentz symmetry is discussed only via continuum embeddings; no discrete boost invariance is claimed.

- The choice of phase/action functional (e.g. Dyck area) is not shown to be unique.

These limitations reflect a deliberate restriction of scope. The goal has been to isolate the minimal recursive structure common to multiple domains, not to provide a complete physical theory.

6.1 Relation to discrete quantum gravity

Similar scaling behavior appears in two-dimensional quantum gravity and random surface models. In particular, Causal Dynamical Triangulations (CDT) enforce a preferred foliation and causal constraint that parallels the prefix order of Dyck paths [2, 3]. In CDT, the continuum limit is taken after summing over causally admissible triangulations. Here the admissible structures are Dyck paths rather than triangulations, but the organizing principle—the restriction to histories that respect a causal growth rule—is closely analogous.

7 Conclusion

This paper treats the Catalan family—Dyck paths, full binary trees, and balanced-parenthesis expressions—as a single discrete history space supporting three complementary readings: causal geometry via the prefix order, computation via application trees and local rewrites, and amplitudes via coherent summation over coarse-grained outcomes. Classical scaling results for conditioned walks provide a continuum comparison in which Dyck ensembles converge to Brownian excursions and the diffusion limit is governed by the heat operator on the half-line; under analytic continuation one obtains the free Schrödinger equation. The scope is intentionally restricted to this shared structural core: deriving interactions, constants, or a unique collapse/measurement rule requires additional structure beyond what is developed here.

A   Coordinate Charts and Continuum Comparisons

This appendix collects optional coordinate embeddings and continuum comparisons used for intuition; the combinatorial results in the main text do not depend on these constructions.

A.1   Coordinate charts on the Catalan cone

Remark A.1 (Notation hygiene). *To avoid collisions, the* tier *(semilength) of a completed history is denoted by n. A* prefix length *is denoted by $k \in \{0, 1, \ldots, 2n\}$. Within this subsection only, the symbols (t_k, x_k) denote an* embedded *spacetime chart derived from cumulative counts (Definition A.1), and should not be confused with the tier index n used elsewhere.*

The Catalan cone as the master object.   Let $\mathcal{C}$ denote the set of Dyck prefixes (balanced-parentheses *prefixes* that never go below height 0), partially ordered by extension: $p \preceq q$ iff q has prefix p. A completed history is a maximal element $w \in \mathcal{D}_n \subset \mathcal{C}$ of semilength n. For any prefix $p \in \mathcal{C}$, the future

$$\mathcal{C}(p) := \{\, q \in \mathcal{C} : p \preceq q \,\}$$

is canonically a "local cone" rooted at p: the same growth law, re-centered. Thus there is a single substrate $\mathcal{C}$ (and its re-rootings), and different "cones" arise from different coordinate charts or coarse-grainings of this same object.

Two cumulative counts and a light-cone chart.   The most rigid chart on $\mathcal{C}$ is obtained by tracking the cumulative numbers of opens and closes.

Definition A.1 (Null counts and embedded coordinates). *Fix a Dyck word $w \in \mathcal{D}_n$, and let $w[1{:}k]$ denote its length-k prefix. Define*

$$u(k) := \#\{\, \texttt{(} \ in \ w[1{:}k]\},\qquad v(k) := \#\{\, \texttt{)} \ in \ w[1{:}k]\}.$$

The Dyck admissibility constraint is $u(k) \geq v(k)$ for all k, and completion is $u(2n) = v(2n) = n$. Define the height (frontier) process

$$H(k) := u(k) - v(k) \geq 0,$$

and the embedded "spacetime" coordinates

$$t_k := \frac{u(k) + v(k)}{2} = \frac{k}{2}, \qquad x_k := \frac{u(k) - v(k)}{2} = \frac{H(k)}{2}.$$

Equivalently $u = t_k + x_k$ and $v = t_k - x_k$ (a discrete null-coordinate form).

Under this embedding, each symbol advances time and changes space by one unit (up to the $1/2$ normalization):

$$\texttt{(} : \ (t, x) \mapsto (t + \tfrac{1}{2}, \ x + \tfrac{1}{2}), \qquad \texttt{)} : \ (t, x) \mapsto (t + \tfrac{1}{2}, \ x - \tfrac{1}{2}).$$

Hence the path stays inside the cone $|x_k| \leq t_k$, with the boundary $x_k = 0$ representing zero frontier (no outstanding opens).

Why "return to 0" is not "return to the origin." The completion constraint $H(2n) = 0$ means only that the *imbalance* vanishes: every open has been matched by a close. In spacetime coordinates, the endpoint is

$$(t_{2n}, x_{2n}) = (n, 0),$$

not $(0, 0)$. Thus a history expands monotonically in t (prefix length grows), while the spatial coordinate x is a *frontier variable* that eventually returns to 0 because no unfinished structure may remain at completion.

Pairs, trees, and S-expressions are identical structure. A Dyck word w can be read as a parenthesized S-expression skeleton, and it already *is* a rooted ordered tree: matched parenthesis pairs are nodes; containment defines parent/child; and left-to-right order in the string gives sibling order. For example, $w = (()())$ has one outer pair (the root) containing two inner pairs (two leaves). Under this identification, the height $H(k)$ is the number of currently-open pairs—the size of the *active frontier* of the tree under construction.

Evaluation "return" as frontier discharge. If evaluation is recorded at the level of control (continuations), then entering a subproblem pushes a context frame and finishing it pops that frame. In a well-bracketed evaluation regime, this push/pop trace is Dyck, and the same counts $(u(k), v(k))$ track control events. The embedded coordinate x_k therefore measures continuation depth (pending contexts), and the return to $x = 0$ at termination is the emptying of the continuation stack: no pending contexts remain. Value return is mediated by this control return; the Dyck "return" is fundamentally the discharge of outstanding obligations.

Breadth as a different projection (history-level, not frontier-level). Statistics such as breadth $r(w)$ summarize a *completed* history by the maximum size of a constant-depth slice in its associated tree. This is a coarse-graining of w (many distinct histories share the same (n, r)), and it should be distinguished from the frontier coordinate x_k, which is an instantaneous depth/obligation variable along a single prefix trajectory.

Summary of the two readings. There is one substrate $\mathcal{C}$ (and its re-rooted futures $\mathcal{C}(p)$). Two useful "cone" pictures arise from: (i) the embedded prefix trajectory (t_k, x_k) derived from null counts (pathwise frontier dynamics), and (ii) history-level projections such as $(n, r(w))$ (coarse geometric envelope). The pairs/tree/S-expression view does not introduce a new object; it is an identity of representations of the same Catalan structure.

A.2 Dyck Coordinates, Lorentz Geometry, and Computational Proper Time

Remark A.2 (Indices and coordinate conventions). *Throughout, n denotes the tier (semilength) of a completed Dyck history. Within this subsection, $k \in \{0, 1, \ldots, 2n\}$ denotes a step index along a single history, and m denotes the number of collapse events (local redex contractions) performed by a chosen evaluation strategy.*

A Dyck history $w \in \mathcal{D}_n$ induces the height process $H(k)$ of Definition A.1. The corresponding embedded coordinates are $t_k = k/2$ and $x_k = H(k)/2$, so that each parenthesis advances time by $\frac{1}{2}$ and changes the transverse coordinate by $\pm\frac{1}{2}$:

$$\texttt{(} : (t, x) \mapsto (t + \tfrac{1}{2},\ x + \tfrac{1}{2}), \qquad \texttt{)} : (t, x) \mapsto (t + \tfrac{1}{2},\ x - \tfrac{1}{2}).$$

For any walk with steps $(\Delta t, \Delta x) = (\frac{1}{2}, \pm\frac{1}{2})$ one has the kinematic cone bound $|x_k - x_0| \leq t_k - t_0$. In the Dyck case, the additional constraint is one-sided: $x_k \geq 0$ for all k, together with the endpoint condition $x_{2n} = 0$. Thus Dyck histories occupy the right half of a discrete light cone and return to the axis only at completion.

Introduce discrete null coordinates (compare Definition A.1)

$$u := t + x, \qquad v := t - x.$$

In continuum $(1+1)$-dimensional Minkowski space, a Lorentz boost with rapidity η acts linearly as

$$u' = e^\eta u, \qquad v' = e^{-\eta} v, \tag{3}$$

and transforming back to (t, x) yields the standard Lorentz transformation

$$t' = \gamma(t - v_L x), \qquad x' = \gamma(x - v_L t), \tag{4}$$

where

$$\gamma = \frac{1}{\sqrt{1 - v_L^2}}, \qquad v_L = \tanh \eta,$$

in units $c = 1$. The Minkowski interval

$$ds^2 = dt^2 - dx^2 \tag{5}$$

is invariant under (4). In this sense the step rule supplies a discrete null-step kinematics, while the Dyck constraint supplies the boundary and return conditions selecting the Catalan ensemble. We emphasize that generic nontrivial boosts do not preserve the discrete Dyck lattice itself (the counts u, v are integers), so the Lorentz discussion here is a continuum comparison for the embedded coordinates rather than a discrete symmetry claim.

Computational proper time. A reduction history carries an intrinsic progress parameter given by the count of collapse events. Let m be the number of local redex contractions performed by an evaluation strategy up to a given stage, and define the *computational proper time*

$$\tau := \alpha\, m, \tag{6}$$

where $\alpha > 0$ is the characteristic scale associated with a single collapse. In continuum Minkowski space, a parametrized world-line $(t(s), x(s))$ admits a proper-time functional

$$\left(\frac{d\tau}{ds}\right)^2 = \left(\frac{dt}{ds}\right)^2 - \left(\frac{dx}{ds}\right)^2, \tag{7}$$

which is Lorentz-invariant under (4). In the present discrete setting, Equation (6) is simply a well-defined event-count parameter; the analogy is that collapse count plays the role of a proper-time progress variable along a chosen computational history.

A.3   Projection to Height Dynamics and Correlation Structure

Let $\mathcal{C}$ denote the set of Dyck prefixes, i.e. finite words in $\{(,)\}$ whose height never falls below zero. Each prefix $p \in \mathcal{C}$ has an associated height $h(p) \in \mathbb{Z}_{\geq 0}$ given by the net excess of opening over closing parentheses. Completed Dyck words of semilength n form the subset $\mathcal{D}_n \subset \mathcal{C}$ of prefixes of length $2n$ with $h = 0$.

The Catalan growth rule specifies admissible extensions: from a prefix p, one may append "(" unconditionally, or ")" provided $h(p) > 0$. To describe this probabilistically, it is convenient to separate the base process from the Dyck-conditioned ensemble.

Base height process. Let $(H_t)_{t \geq 0}$ be a simple symmetric random walk on $\mathbb{Z}$ with increments ± 1. This walk is time-homogeneous and Markov. Its sample paths may be viewed as unconstrained height sequences, without regard to the Dyck condition.

Dyck conditioning. The Dyck ensemble of length $T = 2n$ is obtained by conditioning the base walk on the event

$$\{H_t \geq 0 \text{ for all } t \leq T, \ H_T = 0\}.$$

Under this conditioning, the law of $(H_t)_{t=0}^T$ is uniform on Dyck paths of semilength n. Equivalently, the conditioned process may be represented via a Doob h-transform (or bridge kernel) of the base walk. In this representation, the height process remains Markov but becomes time-inhomogeneous due to the global conditioning. Each completed Dyck word $p \in \mathcal{D}_n$ corresponds uniquely to a sample path

$$(h_0, h_1, \ldots, h_T), \qquad h_0 = h_T = 0, \ h_t \geq 0,$$

drawn from this conditioned law.

Correlation structure. Consider the ensemble of height paths of fixed length T, distributed according to the Dyck-conditioned law. Define the mean and covariance functions

$$\mu_t := \mathbb{E}[H_t], \qquad C(s,t) := \mathbb{E}[(H_s - \mu_s)(H_t - \mu_t)], \qquad 0 \leq s, t \leq T.$$

The covariance kernel C is a symmetric positive operator on the finite-dimensional space $\mathbb{R}^{T+1}$ and captures the second-order temporal structure induced by the Dyck constraint. It admits an eigen-decomposition

$$\sum_{t=0}^T C(s,t) \, v_t^{(k)} = \lambda_k \, v_s^{(k)},$$

yielding an orthogonal family of temporal modes. Any centered height profile admits the expansion

$$H_t - \mu_t = \sum_k \xi_k \, v_t^{(k)}, \qquad \mathbb{E}[\xi_k \xi_\ell] = \lambda_k \, \delta_{k\ell}.$$

In this precise sense, the eigenvalues λ_k constitute the spectrum of temporal correlations induced by the Dyck-conditioned dynamics, and the associated eigenvectors provide a canonical modal decomposition (Karhunen–Loève expansion) of Dyck height signals.

Scaling limit. Under diffusive scaling, the base random walk converges to Brownian motion on $\mathbb{R}$. The Dyck-conditioned law converges to Brownian excursion, which may be described equivalently as Brownian motion conditioned to remain nonnegative and return to zero, or via a Doob transform / Bessel-bridge representation [17, 14]. The resulting continuum evolution is governed by a second-order differential operator on $\mathbb{R}_{\geq 0}$ whose drift and boundary behavior encode the conditioning. In related unconditioned or bridge settings, the associated covariance eigenfunctions are explicitly sinusoidal; for the excursion case, the exact eigenstructure is more subtle, though the dominant modes often resemble sine-like functions away from boundaries.

Thus, the appearance of modal structure follows directly from the projection of Catalan growth dynamics to the height observable and the standard spectral analysis of the resulting correlation kernel, without the introduction of additional physical assumptions.

Remark A.3 (Self-similarity and reference frames). *The Dyck prefix structure is recursively self-similar: every prefix is itself the root of a complete Catalan subtree. Consequently, distinctions such as parent and child, past and future, or global and local history are not intrinsic to the substrate but arise only after fixing a reference root, which induces a causal orientation. The projected height dynamics, their conditioning, and their scaling limits are invariant under such re-rootings.*

B   Additional Technical Notes

B.1   Entropy of coarse-graining and information rate

Fix a tier n and an observable (deterministic coarse-graining) $f : \mathcal{D}_n \to \mathcal{X}$. For $x \in \mathcal{X}$ write

$$N(x) \ := \ \#\{w \in \mathcal{D}_n : f(w) = x\},$$

so that $f^{-1}(x)$ is the equivalence class of histories identified as the same outcome.

Multiplicity entropy.   Define the (microcanonical) entropy of the full ensemble at tier n by

$$S_n \ := \ \log \#(\mathcal{D}_n),$$

and the conditional entropy of an outcome x by

$$S(x) \ := \ \log N(x).$$

The information eliminated by selecting outcome x is the entropy drop

$$\Delta S(x) \ := \ S_n - S(x) \ = \ \log\Big(\frac{\#(\mathcal{D}_n)}{N(x)}\Big).$$

(Any logarithm base may be used; base 2 yields units of bits.)

Information rate as rate of possibility reduction.   Let m denote the number of selection events (local contractions) along a history, and let computational proper time be $\tau = \tau_0 m$ for a fixed scale $\tau_0 > 0$. We define the information rate associated with outcome x to be the information loss per unit computational proper time,

$$R(x) \ := \ \frac{\Delta S(x)}{\tau}.$$

In the simplest case of a single event ($m = 1$), this reduces to $R(x) = \Delta S(x)/\tau_0$.

Gauge-invariant counting.   When histories admit a redundancy under commuting spacelike-separated updates, one may quotient $\mathcal{D}_n$ by the induced gauge equivalence relation $\sim_g$ and define $\bar{\mathcal{D}}_n := \mathcal{D}_n/\sim_g$. If f is gauge-invariant (constant on $\sim_g$-orbits), define

$$\bar{N}(x) := \#\{[w] \in \bar{\mathcal{D}}_n : f(w) = x\}, \qquad \bar{\Delta S}(x) := \log\Big(\frac{\#(\bar{\mathcal{D}}_n)}{\bar{N}(x)}\Big),$$

and use $\bar{\Delta}S$ in place of ΔS. This removes overcounting due solely to reordering of independent collapses.

C A Double-Slit Thought Experiment on the Catalan Light Cone

This appendix provides an illustrative thought experiment showing how the discrete path-integral formalism developed in Section 4 exhibits interference in a setting analogous to the double-slit experiment. The construction is entirely combinatorial and finite. No new assumptions, dynamical rules, or continuum limits are introduced; the purpose is solely to instantiate the formalism in a familiar narrative.

C.1 Two sources as boundary-conditioned cones

Consider two distinct Dyck prefixes u_L and u_R of equal length and height. Each prefix induces a local Catalan cone of admissible continuations, as described in Section 2.9. We refer to these as the left and right source cones, although no spatial interpretation is assumed at this stage.

Both cones are evolved to a common tier n, producing two ensembles of Dyck paths of semilength n that differ only in their initial boundary condition. The admissible histories from both cones are evaluated relative to the same observable defined below.

C.2 Observable and indistinguishability

Fix a tier n and define an observable

$$f : \mathcal{D}_n \to \mathcal{X},$$

where $\mathcal{X}$ is a discrete outcome space. The observable f retains a coarse-grained feature of each history (for example, a bin determined by the mean height or total area) and discards all other information, including which source cone the history originated from.

Interference arises precisely because histories originating from distinct cones may be rendered indistinguishable by the observable. If the observable were to retain source information, no interference would occur.

C.3 A worked finite example

Take $n = 4$ and choose two admissible Dyck prefixes of equal length and height,

$$u_L = \texttt{(()(}, \qquad u_R = \texttt{()((},$$

each of length 4 and height 2. Each prefix admits exactly three completions to a full Dyck word of length 8, yielding six histories in the union of the two source cones.

Define a coarse observable that discards source information by sampling the height at a fixed time step after the "slits":

$$f(w) := H_w(6) \in \{0, 2\}.$$

This is a discrete analogue of recording transverse displacement at a detector time without access to which slit was taken.

With phase $\psi(w) = e^{i\alpha A(w)}$, the detector amplitudes are

$$\Psi(2) = \sum_{f(w)=2} e^{i\alpha A(w)} = e^{i12\alpha} + 2e^{i10\alpha} + e^{i8\alpha} = 2e^{i10\alpha}\big(1 + \cos(2\alpha)\big),$$

$$\Psi(0) = \sum_{f(w)=0} e^{i\alpha A(w)} = e^{i8\alpha} + e^{i6\alpha} = 2e^{i7\alpha}\cos(\alpha).$$

cone	w	$A(w)$	$f(w) = H_w(6)$
L	(()(()))	12	2
L	(()()())	10	2
L	(()())()	8	0
R	()((()))	10	2
R	()(()())	8	2
R	()(())()	6	0

Table 1: Two equal-height source cones at $n = 4$ and a coarse detector observable.

Classically one would predict multiplicities $N(2) = 4$ and $N(0) = 2$. In contrast, the quantum intensities $|\Psi(x)|^2$ vary with α and can exhibit strong suppression. For example, at $\alpha = \pi/2$ one obtains $\Psi(2) = 0$ (exact destructive interference at the outcome $x = 2$), even though $N(2) = 4$ histories contribute.

This example is intentionally tiny: its purpose is to show, in finite combinatorial terms, how (i) multiple histories per outcome, (ii) an additive phase functional, and (iii) coarse observation together produce interference. Larger n yields richer outcome sets and more intricate cancellation patterns.

C.4   Summary

No wave equation, spatial geometry, or continuum approximation is assumed in this construction. The example simply instantiates the general mechanism of Section 4: complex weights, coherent summation over coarse-grained preimages, and Born-style squaring suffice to produce interference.

D   Computational Foundations

This appendix records proof sketches for the computational claims used in the main text, including Proposition 3.1 and the disjoint-commutation property of Lemma D.2. For a lean v1, extended examples and additional formal development are omitted.

Lemma D.1 (Internalizing Symbols as Motifs)**.** *Let Σ be a finite (or countable) alphabet of atomic symbols, and consider finite applicative terms over Σ (binary application with atoms). There is an injective encoding of such labeled application trees into the Catalan family $\mathcal{C}$ of unlabeled full binary trees. One explicit construction fixes two distinct tag trees $A, B \in \mathcal{C}$, assigns each $\sigma \in \Sigma$ a distinct motif $S_\sigma \in \mathcal{C} \setminus \{A, B\}$, and defines*

$$E(\sigma) := \bullet(A, S_\sigma), \qquad E(t \cdot u) := \bullet\big(B, \bullet(E(t), E(u))\big),$$

where $t \cdot u$ denotes application and $\bullet(\cdot, \cdot)$ denotes binary pairing of subtrees. The left tag distinguishes atoms from applications, so E is recursively decodable and therefore injective.

Proof Sketch (of Proposition 3.1). As described in classical treatments of combinatory logic and the λ-calculus [8, 4], application is a binary operation, and every term therefore possesses a unique representation as a full binary tree: internal nodes encode application, and leaves encode variables, constants, or combinators. This establishes a canonical embedding of programs into $\mathcal{C}$.

Conversely, any full binary tree with labeled leaves may be interpreted as a well-formed program term by reading internal nodes as applications and leaves as atomic symbols, yielding a unique term up to α-equivalence.

Operational semantics are defined via local tree rewrites. A β-redex $(\lambda x.M)\,N$ contracts by replacing the parent application with $M[x := N]$; SKI reductions replace specific subtrees according to fixed patterns. In each case, the output remains a full binary tree, so evaluation never leaves $\mathcal{C}$. Because nondeterministic redex choices correspond to branching in the space of trees, each complete reduction sequence is a path through the Catalan possibility space, completing the correspondence. $\square$

Lemma D.2 (Commutation of disjoint reductions). *Let T be a full binary tree and consider any local rewrite system whose single-step reductions replace a rooted subtree matching a finite pattern by a new subtree, leaving the rest of T unchanged. Suppose two single-step reductions are applicable at positions p and q whose rooted subtrees are disjoint (neither position lies on the root-to-node path of the other). Let T_p denote the result of applying the reduction at p, and similarly T_q. Then both reductions remain applicable after the other, and they commute:*

$$(T_p)_q \;\equiv\; (T_q)_p.$$

In particular, disjoint reductions form a commuting diamond as in Figure 6.

Proof Sketch. Since p and q lie in disjoint subtrees, contracting at p rewrites only the subtree rooted at p and leaves the subtree rooted at q unchanged. Symmetrically, contracting at q leaves the subtree at p unchanged. Because the two rewrite steps act on disjoint parts of the tree, performing both contractions yields the same result regardless of order. $\square$

References

[1] L. Addario-Berry, L. Devroye, and S. Janson. Sub-Gaussian tail bounds for the width and height of conditioned Galton–Watson trees. *Annals of Probability*, 41(2):1074–1087, 2013.

[2] J. Ambjørn, J. Jurkiewicz, and R. Loll. Dynamically triangulating Lorentzian quantum gravity. *Nuclear Physics B*, 610:347–382, 2001.

[3] J. Ambjørn, A. Görlich, J. Jurkiewicz, and R. Loll. Nonperturbative quantum gravity. *Physics Reports*, 519:127–210, 2012.

[4] H. P. Barendregt. *The Lambda Calculus: Its Syntax and Semantics*. North-Holland, 1984.

[5] L. Bombelli, J. Lee, D. Meyer, and R. D. Sorkin. Space-time as a causal set. *Physical Review Letters*, 59(5):521–524, 1987.

[6] A. Church. A set of postulates for the foundation of logic. *Annals of Mathematics*, 34:839–864, 1933.

[7] T. M. Cover and J. A. Thomas. *Elements of Information Theory*. 2nd edition, John Wiley & Sons, 2006.

[8] H. B. Curry and R. Feys. *Combinatory Logic, Vol. I*. North-Holland, 1958.

[9] R. P. Feynman and A. R. Hibbs. *Quantum Mechanics and Path Integrals*. McGraw–Hill, 1965. (Dover reprint, 2010).

[10] S. Janson. Brownian excursion area, Wright's constants in graph enumeration, and other Brownian areas. *Probability Surveys*, 4:80–145, 2007.

[11] M. Kac. On distributions of certain Wiener functionals. *Transactions of the American Mathematical Society*, 65(1):1–13, 1949.

[12] J.-F. Le Gall. Random trees and applications. *Probability Surveys*, 2:245–311, 2005.

[13] R. Orús. A practical introduction to tensor networks: Matrix product states and projected entangled pair states. *Annals of Physics*, 349:117–158, 2014.

[14] J. Pitman. Brownian motion, bridge, excursion, and meander revisited. *Electronic Journal of Probability*, 4:1–32, 1999.

[15] C. Rovelli. *Quantum Gravity*. Cambridge University Press, 2004.

[16] R. P. Stanley. *Catalan Numbers*. Cambridge University Press, 2015.

[17] L. Takács. A Bernoulli excursion and its various applications. *Advances in Applied Probability*, 23(3):557–585, 1991.